RAPID COMMUNICATION

Forming solid electrolyte interphase *in situ* in an ionic conducting $Li_{1.5}Al_{0.5}Ge_{1.5}(PO_4)_3$-polypropylene (PP) based separator for Li-ion batteries*

Jiao-Yang Wu(吴娇杨)[1], Shi-Gang Ling(凌仕刚)[1], Qi Yang (杨琪)[1], Hong Li(李泓)[1,†], Xiao-Xiong Xu(许晓雄)[2], and Li-Quan Chen(陈立泉)[1]

[1] *Beijing National Laboratory for Condensed Matter Physics, Institute of Physics, Chinese Academy of Sciences, Beijing* 100190, *China*
[2] *Ningbo Institute of Material Technology Engineering, Chinese Academy of Sciences, Zhejiang* 315201, *China*

(Received 13 April 2016; revised manuscript received 20 April 2016; published online 1 June 2016)

A new concept of forming solid electrolyte interphases (SEI) *in situ* in an ionic conducting $Li_{1.5}Al_{0.5}Ge_{1.5}(PO_4)_3$-polypropylene (LAGP-PP) based separator during charging and discharging is proposed and demonstrated. This unique structure shows a high ionic conductivity, low interface resistance with electrode, and can suppress the growth of lithium dendrite. The features of forming the SEI *in situ* are investigated by scanning electron microscopy (SEM) and x-ray photoelectron spectroscopy (XPS). The results confirm that SEI films mainly consist of lithium fluoride and carbonates with various alkyl contents. The cell assembled by using the LAGP-coated separator demonstrates a good cycling performance even at high charging rates, and the lithium dendrites were not observed on the lithium metal electrode. Therefore, the SEI-LAGP-PP separator can be used as a promising flexible solid electrolyte for solid state lithium batteries.

Keywords: solid state lithium batteries, solid electrolyte interphase, ionic conductor coated separator, lithium dendrite

PACS: 82.47.Aa, 65.40.gk, 82.45.Fk **DOI:** 10.1088/1674-1056/25/7/078204

1. Introduction

Energy and environment are the two serious issues, therefore developing clean and renewable energy resources is our urgent work.[1] Lithium ion batteries (LIBs) are a kind of green energy battery which represents the future development direction. It has been widely used in portable electronic devices, electric vehicles, and stationary type distributed power sources.[2] However, conventional lithium ion batteries with flammable non-aqueous electrolytes have safety risks. Nevertheless, solid state lithium ion batteries are considered to be the ultimate solution for improving the safety performance.[3] In order to satisfy large scale manufacturing, many efforts are paid to fabricate solid electrolytes which have both the flexible feature and good electrochemical properties.[4]

Polymer electrolytes, polymer-inorganic composite electrolytes, and inorganic ceramic electrolytes are developed as solid electrolytes systems. High molecular weight polymer hosts have been studied, especially for the poly(ethylene oxide) (PEO)-based polymer electrolytes. However, in the dry solid polymer electrolyte system (PEO–LiX), it exhibits very low ionic conductivity on the order of 10^{-6} S·cm^{-1} at room temperature.[5] This lower conductivity excludes this type of membrane from practical applications at room temperature. The most common approach to enhance the conductivity of dry solid polymer electrolyte is to add inorganic nano-particles into the polymer host. The ceramic fillers are generally divided into two categories: inactive fillers that are not involved in the lithium ion conduction process (e.g., Al_2O_3[6] and SiO_2[7]) and active ones that participate in lithium ion transport (e.g., Li_3N[8] and $Li_7La_3Zr_2O_{12}$[9]). Croce *et al.*[10] reported the conductivities of a PEO–$LiClO_4$ mixture containing nano-powders of TiO_2 and Al_2O_3 can reach 10^{-4} S·cm^{-1} at 50 °C and 10^{-5} S·cm^{-1} at 30 °C, respectively. However, with the addition of inorganic nano-particles, it accelerated deterioration of the electrolyte's mechanical properties.[9] Kamaya *et al.*[11] reported a lithium superionic conductor $Li_{10}GeP_2S_{12}$ that had a new three-dimensional framework structure. It exhibited an extremely high lithium ionic conductivity of 1.2×10^{-2} S·cm^{-1} at room temperature. While the sulfide electrolytes are not stable in the air, it can react with water and produce poisonous gas. Also inorganic ceramic is not flexible compared with polymer and is fragile, which is much more difficult to handle than polymer-based solid membranes.[12] Luo *et al.*[13] found that a 4–5 μm thick solid electrolyte interphase (SEI) layer could be formed on a well-defined silicon nanocone surface. This SEI layer can be used as a composite solid electrolyte for solid lithium batteries.

Recently, Xu *et al.*[14] reported an ionic conductor $Li_{1.5}Al_{0.5}Ge_{1.5}(PO_4)_3$ (LAGP) coated on the surface of a PP separator. In contrast with other inorganic coatings, such as

*Project supported by the Beijing Science and Technology Project, China (Grant No. Z13111000340000), the National Basic Research Program of China (Grant No. 2012CB932900), and the National Natural Science Foundation of China (Grant Nos. 51325206 and 51421002).

†Corresponding author. E-mail: hli@iphy.ac.cn

© 2016 Chinese Physical Society and IOP Publishing Ltd

Al_2O_3, TiO_2, ZnO, and ZrO_2,[15,16] LAGP is an excellent lithium ion conductor, which allows the rapid diffusion of lithium ion through the coating layer. Therefore, it could reduce the ionic resistance compared to the inert ceramic coated separator.[17,18] The coating layer LAGP helps to give a high ion conductivity. Besides, the cell assembled by using the LAGP coating separator shows a superior rate capability and cycle ability in high-voltage cathode materials up to 5 V. For this type of ionic conductor coated separator (ICCS), the ionic conductor exists as contacted particles and the high ionic conductivity in bulk phase may not be useful.

Herein, the authors propose a new strategy by *in-situ* growing SEI on the surface of ionic conducting $Li_{1.5}Al_{0.5}Ge_{1.5}(PO_4)_3$-polypropylene based (LAGP-PP) separator for the first time. With the decomposition of electrolytes during the charge/discharge process, the SEI layer formed on the LAGP-PP separator became thicker and thicker, and the artificial SEI-LAGP-PP structure was obtained eventually. This structure has the functionality of a solid electrolyte layer, i.e., preventing electronic conduction but providing lithium ion conducting properties as an electrolyte.[19–21] The separator shows excellent ionic conductivity, good cycling performance, and high rate capability. The morphology and composition of the artificial SEI-LAGP-PP structure and the surface morphology of Li electrode are explored and discussed.

2. Experiment

The LAGP-PP separator was reported by Xu *et al.*[14] The cathode was a commercial product with a composition of $LiCoO_2$, conductive acetylene black, and polyvinylidene-fluoride (PVDF KynarFlex 2801, Atochem) at a weight ratio of 93:4:3 (Amperex Technology Limited). The cathode sheets with dimensions of 8 mm×8 mm were prepared, and kept in a 120 °C oven for 6 h. The active material loading was 16.625 mg·cm^{-2}. The liquid electrolyte was composed of 1M $LiPF_6$ in ethylene carbonate (EC) and dimethyl carbonate (DMC) (1:1 by volume) with vinylene carbonate (VC) as the film-forming additive (2 wt%).

The CR2032 coin cells were assembled in an argon gas filled glove box (H_2O and $O_2 < 0.1$ ppm). The charge/discharge cycling performances were measured at room temperature using a Land BT2000 Battery Test System (Wuhan, China) in the voltage range of 3 V–4.2 V under 0.1C, 0.5C, 1C rates, corresponding to 0.23 mA·cm^{-2}, 1.16 mA·cm^{-2}, and 2.33 mA·cm^{-2} current density, respectively.

The Li/LAGP-PP/$LiCoO_2$ cells were disassembled in an argon gas filled glove box after 10 cycles (0.1C), 380 cycles (0.5C), and 450 cycles (1C), respectively. The separators and Li electrodes were taken out of the cells and washed with anhydrous DMC more than three times. The washed separators and Li electrodes were dried in the vacuum chamber of the glove box for at least 6 h for further test.

Three different separators were labeled as (i) pristine dry LAGP-PP separator, (ii) LAGP-PP separator after 380 cycles in Li/LAGP-PP/$LiCoO_2$ cell at 0.5C, (iii) LAGP-PP separator soaked in the liquid electrolyte. The bulk impedance (R_b) was measured at room temperature by the Zahner IM6 electrochemical analyzer with an ac oscillation voltage of 5 mV in the frequency range from 1 Hz to 8 MHz. Each separator was sandwiched between a pair of stainless steel blocking electrodes of diameter 10 mm. The ion conductivity (σ) is calculated by

$$\sigma = \frac{d}{R_b S}, \tag{1}$$

where d and S are the thickness and effective area of separators (i), (ii), (iii), respectively.

The cyclic voltammetry (CV) was tested on a CHI627D electrochemical analyzer using a CR2032 cell. In the Li/LAGP-PP/$LiCoO_2$ cell, metallic lithium was used as the anode. The cutting-off voltage range was 3 V–4.2 V. The testing temperature was room temperature and the scanning rate was 1 mV/s.

The crystal structure of the pristine LAGP-PP separator was measured using a Bruker D8 Advance diffractometer with Cu Kα radiation at a scanning rate of 0.5° min^{-1} in the 2θ range of 10°–44°. The surface and cross-section morphologies of the LAGP-PP separator and Li electrode were analyzed using the SEM (HITACHI S4800). XPS data was obtained using an ESCALab250 electron spectrometer with monochromatic Mg Kα radiation, and specific correction was conducted by using C 1s binding energy of 284.6 eV.

3. Results and discussion

Figure 1 shows the XRD patterns of the pristine LAGP-PP separator. The pattern has a minor impurity peak corresponding to SiO_2,[22] which should be attributed to the penetration effect of x-ray through the separator on the sample stage. The peaks match well with the PDF card of $LiGe_2(PO_4)_3$ broad bands and no obvious shift of the peaks can be observed, although 25% of Ge^{4+} in $LiGe_2(PO_4)_3$ are substituted by Al^{3+}. This is due to the similarity of ionic radius between Ge^{4+} (0.053 nm) and Al^{3+} (0.050 nm).[23] Also the patterns show broad bands, indicating the glass nature of the LAGP.

Figure 2(a) shows the cyclic voltammetry curve of the Li/LAGP-PP/$LiCoO_2$ cell of the first cycle. A pair of oxidation and reduction current peaks is observed at 4.1 V and 3.81 V, respectively, corresponding to the deintercalation and intercalation of Li^+ from the $LiCoO_2$ cathode. The LAGP-PP separator is stable in the scope of 2.9 V–4.2 V.

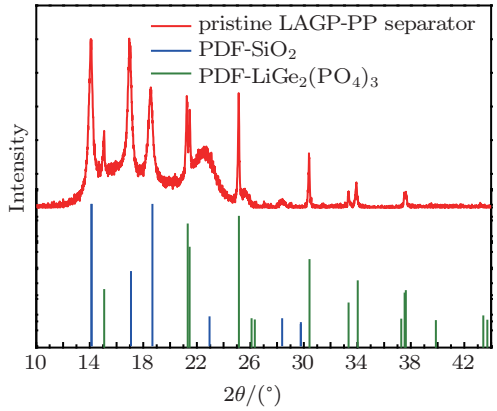


Fig. 1. (color online) XRD patterns of the pristine LAGP-PP separator.

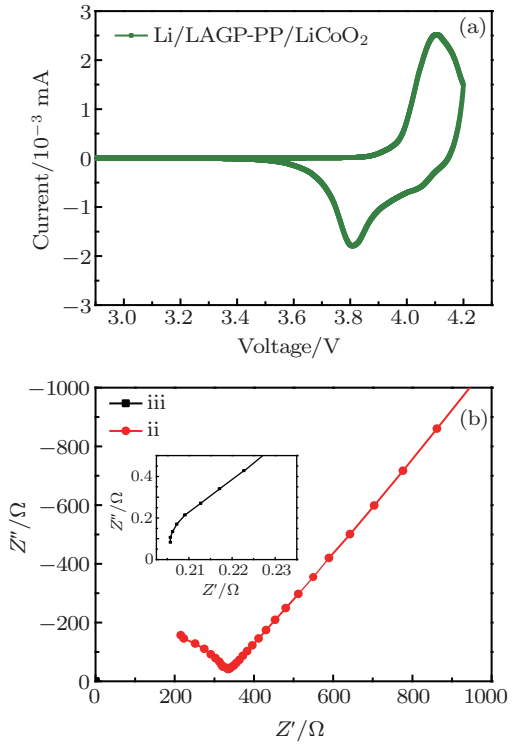


Fig. 2. (color online) (a) Cyclic voltammetry curve of Li/LAGP-PP/$LiCoO_2$ cell at a scan rate of 1 $mV{\cdot}s^{-1}$. (b) Impedance spectra of (ii) LAGP-PP separator after 380 cycles in Li/LAGP-PP/$LiCoO_2$ cell at 0.5C (iii) LAGP-PP separator soaked in the liquid electrolyte.

The ion conductivities of separators (i), (ii), (iii) are compared below. The impedances of (ii) and (iii) are shown in Fig. 2(b). The ion conductivities of (ii) and (iii) were 1.5×10^{-5} $S{\cdot}cm^{-1}$ and 1.4×10^{-2} $S{\cdot}cm^{-1}$, respectively. Also, the conductivity of separator (i) was measured, but the conductivity was too low ($< 10^{-9}$ $S{\cdot}cm^{-1}$) and beyond the range of Zahner IM6. Although the conductivity of solid separator (ii) is less than liquid separator (iii), its order of magnitude is the same as polymer electrolytes. These results encourage us that the dry SEI-LAGP-PP separator can be designed as solid electrolytes due to its acceptable conductivity. As the SEI-LAGP-PP separator was *in-situ* formed, it has good mechanical properties and excellent interface properties with the electrode.

Figure 3 presents the rate capability of Li/LAGP-PP/$LiCoO_2$ cell at 0.1C, 0.5C, 1C, respectively. The initial discharge capacity was 145.3 $mAh{\cdot}g^{-1}$. The capacity retention can be maintained at 75.8% after 150 cycles at a 0.1C rate. Even at the 1C rate, the cell has better Coulombic efficiency, with a discharge capacity of 73.3 $mAh{\cdot}g^{-1}$ after 400 cycles. This is due to the fact that the dense artificial SEI were formed on the LAGP particles' surface, and these stable artificial SEIs could prevent some side reactions at the interfacial layer.

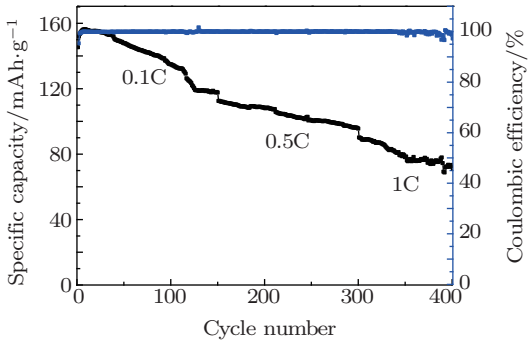


Fig. 3. (color online) The rate capacity under variable current rate of the Li/LAGP-PP/$LiCoO_2$ cell.

Figure 4 displays the surface morphologies of LAGP-PP separator corresponding to 0 cycle, 10 cycles (0.1C), 380 cycles (0.5C), 450 cycles (1C), respectively. The SEM images of the fresh LAGP-PP separator agree well with Xu's work.[14] It is obvious that the separator is coated with LAGP particles, and the size of the particles is about 0.5 μm–1 μm (Fig. 4(a)). After 10 cycles, the surface morphologies of the LAGP-PP separator changed partially, seeming to be covered by a thin film, so-called an SEI film in the inset of Fig. 4(b). At some other areas, the SEI films were not formed, and LAGP particles were naked (Fig. 4(b)). After 380 cycles (0.5C) and 450 cycles (1C), no LAGP particles can be seen from the top view and both surfaces were covered by SEI films completely (Figs. 4(c) and 4(d)). After long cycles, the cavities between LAGP particles were filled with SEI film densely. The separator converted into an ionic conductivity separator eventually.

In order to observe more directly, the cross section morphologies are also shown in Fig. 5. It shows that LAGP particles were wrapped by artificial SEI with a leaf-like morphology after 10 cycles (Fig. 3(b)), which is quite different from the pristine separator (Fig. 5(a)). This unique surface structure confirms that the artificial SEI films formed on the ionic conductor LAGP particles surface during the cycling process. After 380 cycles (0.5C) and 450 cycles (1C), the LAGP particles were coated with SEI films densely and homogenously (Figs. 5(c) and 5(d)). The cross section morphologies are in agreement with the surface ones.

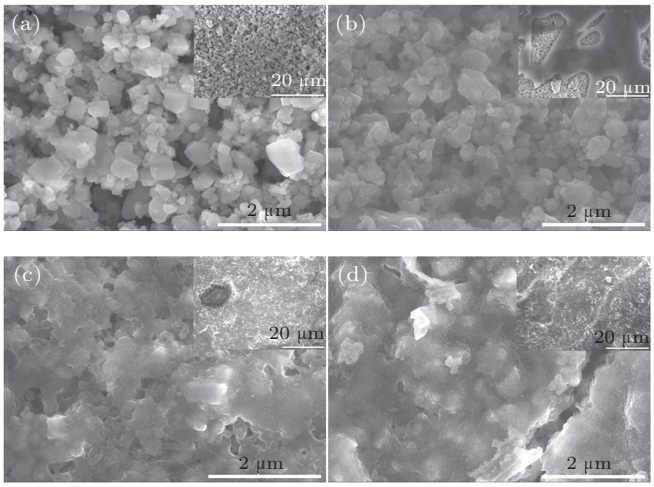


Fig. 4. (color online) SEM images of LAGP-PP separators surface after different cycles in Li/separator/$LiCoO_2$ cell. (a) 0 cycle, (b) 10 cycles at 0.1C, (c) 380 cycles at 0.5C, and (d) 450 cycles at 1C.

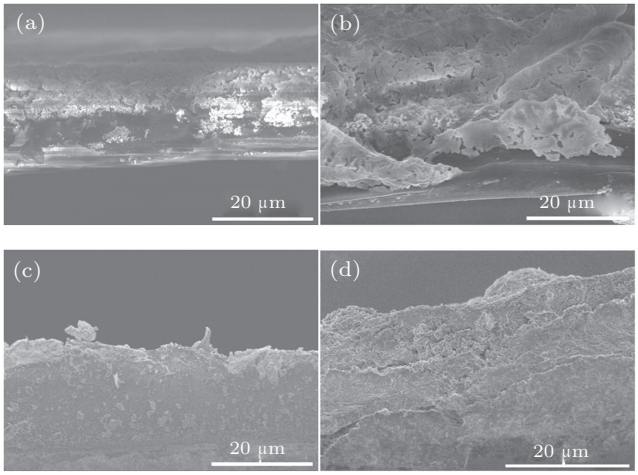


Fig. 5. (color online) SEM images of LAGP-PP separators cross section after different cycles in Li/separator/$LiCoO_2$ cell. (a) 0 cycle, (b) 10 cycles at 0.1C, (c) 380 cycles at 0.5C, and (d) 450 cycles at 1C.

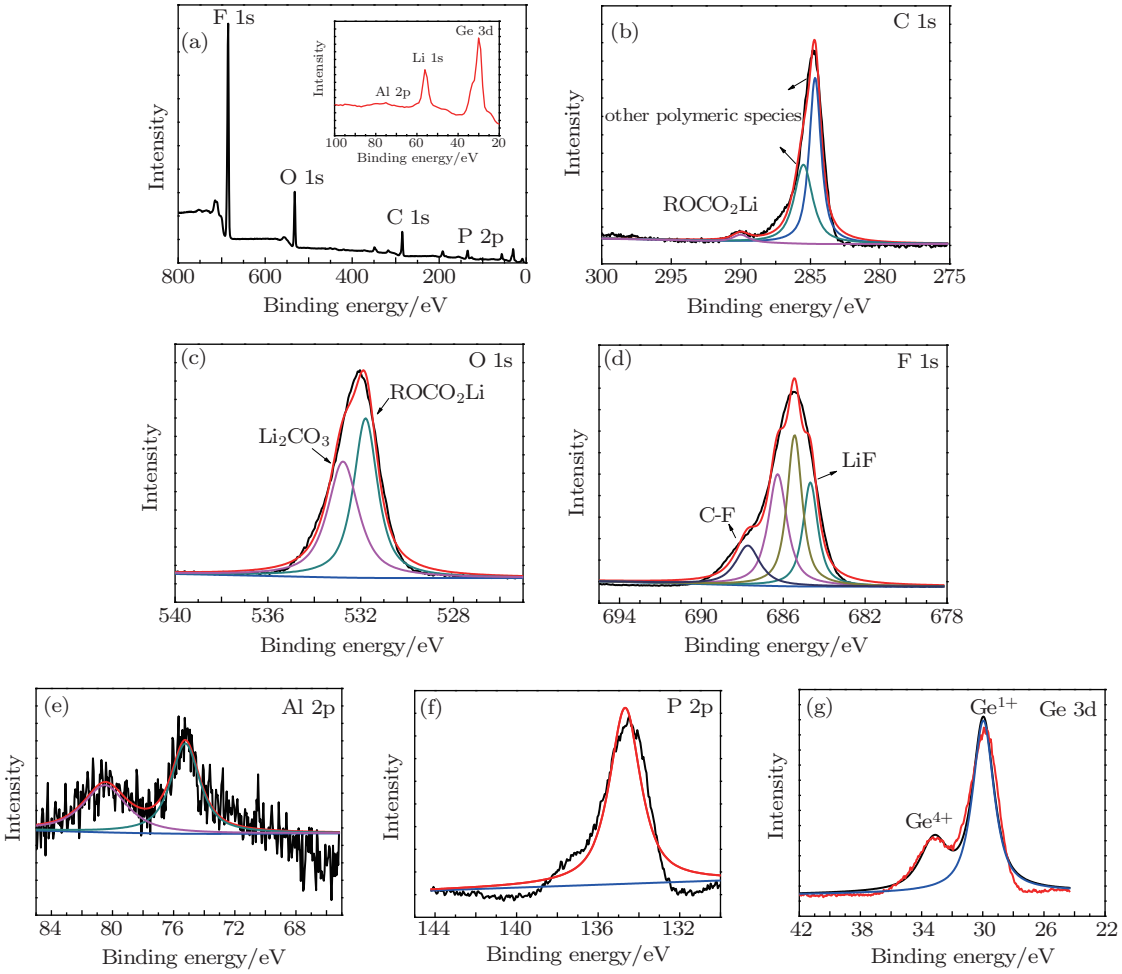


Fig. 6. (color online) XPS spectra of LAGP-PP separator surface after 10 cycles in Li/separator/$LiCoO_2$ cell at 0.1C. XPS spectra of (a) LAGP-PP separator surface, (b) C 1s, (c) O 1s, (d) F 1s, (e) Al 2p, (f) P 2p, and (g) Ge 3d.

The surface compositions of the LAGP-PP separator in the Li/LAGP-PP/$LiCoO_2$ cell after 10 cycles were further investigated by XPS, as shown in Fig. 6. The C 1s peaks of 290.0 eV would be assigned to $ROCO_2Li$, 284.6 eV and 285.5 eV peaks to other polymeric species.[24] The O 1s peaks of 531.8 eV and 532.8 eV are assigned to $ROCO_2Li$ and Li_2CO_3, respectively.[25,26] The peak around 687.7 eV of F 1s is assigned to the C-F and the 686.3 eV, 685.4 eV, 684.6 eV peaks to LiF.[27] All the results confirmed that the uniform SEI films typically consist of lithium fluoride and carbonates with

various alkyl contents. It is observed that the Ge 3d peaks appear at 29.9 eV and 33.1 eV, corresponding to Ge^{1+} and Ge^{4+},[28,29] respectively. The reduction process can be due to the reaction of LAGP with metallic lithium, which results in the reduction of Ge valence and LAGP converting from the pure ionic conductor to the mixed conductor. Therefore, the continuous growth of SEI could be possible on the surface of LAGP particles and finally formed a dense SEI film on the LAGP-PP separator.

Moreover, this artificial SEI-LAGP-PP structure is able to suppress the lithium dendrite growth effectively. In most of the commonly used non-aqueous electrolyte solutions, Li dendrite is easily formed during the Li deposition at the current density above 1 mA·cm^{-2}.[30] The incompact and dendritic Li can consume much more electrolyte and result in low cycling efficiency.[31] In this experiment even 2.33 mA·cm^{-2} (1C rate) current density was used to observe the surface morphology of Li deposition. The surface morphologies of Li electrodes at 10 cycles (0.1C), 380 cycles (0.5C), and 450 cycles (1C) are shown in Fig. 7. For the cell after 10 cycles at 0.1C, it is obvious to see that the Li electrode surface was flat and smooth, even some LAGP particles of the LAGP-PP separator were adhering to the Li surface (Fig. 7(a)). After cycling for 380 cycles at 0.5C and 450 cycles at 1C, the Li surface exhibits a neat and compact film (Figs. 7(b) and 7(c)), which offers a good condition for forming a high-quality SEI film. The needle-like lithium dendrites were not observed. Therefore, the LAGP-PP separator benefits from forming a uniform and compact SEI layer, and helps to improve the high rate performance of rechargeable Li metal based batteries.

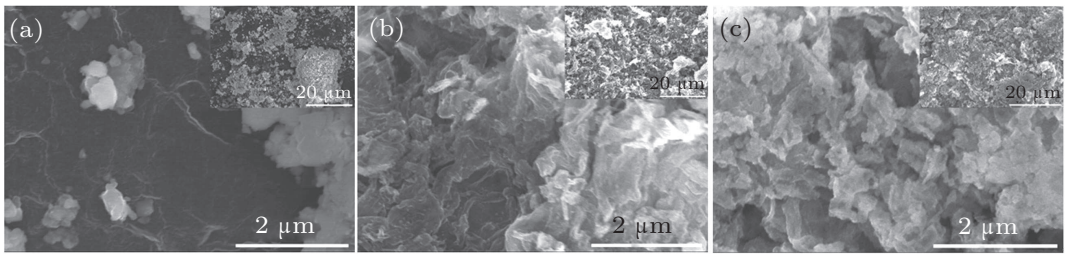


Fig. 7. SEM images of of Li electrodes after different cycles in Li/separator/$LiCoO_2$ cell. (a) 10 cycles at 0.1C, (b) 380 cycles at 0.5C, and (c) 450 cycles at 1C.

4. Conclusion

In summary, the artificial solid electrolyte interphase (SEI) was formed upon cycling on an ionic conductor LAGP coated PP separator. The LAGP particles were wrapped by artificial SEI densely. The ion conductivity of one SEI-LAGP-PP separator was 1.5×10^{-5} S·cm^{-1} at room temperature, which indicates that it can be used as a solid electrolyte. The uniform artificial SEI consists of LiF, Li_2CO_3, and $ROCO_2Li$. The LAGP-PP separator in the Li/$LiCoO_2$ cell exhibited good cycle performances even at the 1C rate. Also this artificial SEI-LAGP-PP structure can effectively suppress the lithium dendrite after 450 cycles at the 1C rate. All the above results prove that this novel LAGP-PP separator can convert into an ionic conducting SEI-LAGP-PP separator. This unique structure has great potential to be used in rechargeable solid lithium batteries.

References

[1] Whittingham M S 2008 *Mrs Bulletin* **33** 411
[2] Arico A S, Bruce P, Scrosati B, Tarascon J M and Van Schalkwijk W 2005 *Nat. Mater.* **4** 366
[3] Tarascon J M and Armand M 2001 *Nature* **414** 359
[4] Abraham K M and Jiang Z 1996 *J. Electrochem. Soc.* **143** 1
[5] Quartarone E, Mustarelli P and Magistris A 1998 *Solid State Ion.* **110** 1
[6] Masoud E M, El-Bellihi A A, Bayoumy W A and Mousa M A 2013 *J. Alloy. Compound.* **575** 223
[7] Kim J W, Ji K S, Lee J P and Park J W 2003 *J. Power Sources* **119** 415
[8] Stephan A M and Nahm K S 2006 *Polymer* **47** 5952
[9] Choi J H, Lee C H, Yu J H, Doh C H and Lee S M 2015 *J. Power Sources* **274** 458
[10] Croce F, Appetecchi G B, Persi L and Scrosati B 1998 *Nature* **394** 456
[11] Kamaya N, Homma K, Yamakawa Y, Hirayama M, Kanno R, Yonemura M, Kamiyama T, Kato Y, Hama S, Kawamoto K and Mitsui A 2011 *Nat. Mater.* **10** 682
[12] Zhao Y, Wu C, Peng G, Chen X, Yao X, Bai Y, Wu F, Chen S and Xu X 2016 *J. Power Sources* **301** 47
[13] Luo F, Chu G, Xia X, Liu B, Zheng J, Li J, Li H, Gu C and Chen L 2015 *Nanoscale* **7** 7651
[14] Shi J, Xia Y, Han S, Fang L, Pan M, Xu X and Liu Z 2015 *J. Power Sources* **273** 389
[15] Wu Y P, Rahm E and Holze R 2003 *J. Power Sources* **114** 228
[16] Takamura T, Sumiya K, Suzuki J, Yamada C and Sekine K 1999 *J. Power Sources* **81** 368
[17] Hartmann P, Leichtweiss T, Busche M R, Schneider M, Reich M, Sann J, Adelhelm P and Janek J 2013 *J. Phys. Chem. C* **117** 21064
[18] Mariappan C R, Yada C, Rosciano F and Roling B 2011 *J. Power Sources* **196** 6456
[19] Moller K C, Hodal T, Appel W K, Winter M and Besenhard J O 2001 *J. Power Sources* **97** 595
[20] Lu M, Cheng H and Yang Y 2008 *Electrochim. Acta* **53** 3539
[21] Lee S H, You H G, Han K S, Kim J, Jung I H and Song J H 2014 *J. Power Sources* **247** 307
[22] Cannas C, Casu M, Lai A, Musinu A and Piccaluga G 1999 *J. Mater. Chem.* **9** 1765
[23] Inada R, Ishida K I, Tojo M, Okada T, Tojo T and Sakurai Y 2015 *Ceram. Int.* **41** 11136
[24] Bettge M, Li Y, Sankaran B, Rago N D, Spila T, Haasch R T, Petrov I and Abraham D P 2013 *J. Power Sources* **233** 346
[25] Sugimoto T, Kikuta M, Ishiko E, Kono M and Ishikawa M 2008 *J. Power Sources* **183** 436
[26] Howlett P C, Brack N, Hollenkamp A F, Forsyth M and MacFarlane D R 2006 *J. Electrochem. Soc.* **153** A595
[27] Budi A, Basile A, Opletal G, Hollenkamp A F, Best A S, Rees R J, Bhatt A I, O'Mullane A P and Russo S P 2012 *J. Phys. Chem. C* **116** 19789
[28] Wang X, Xiang J, Wang W, Xiong Y, Zhang J and Zhao C 2015 *Appl. Surf. Sci.* **357** 1857
[29] Kato K, Kyogoku S, Sakashita M, Takeuchi W, Kondo H, Takeuchi S, Nakatsuka O and Zaima S 2011 *Jpn J. Appl. Phys.* **50** 10PE02
[30] Aurbach D, Zinigrad E, Teller H, Cohen Y, Salitra G, Yamin H, Dan P and Elster E 2002 *J. Electrochem. Soc.* **149** A1267
[31] Miao R, Yang J, Feng X, Jia H, Wang J and Nuli Y 2014 *J. Power Sources* **271** 291